IEEE Access
Multidisciplinary | Rapid Review | Open Access Journal

Received August 9, 2018, accepted September 14, 2018, date of publication September 28, 2018, date of current version October 19, 2018.

Digital Object Identifier 10.1109/ACCESS.2018.2872788

Optimal Planning of Multiple Distributed Generating Units and Storage in Active Distribution Networks

MUHAMMAD KHALID, (Member, IEEE), UMER AKRAM, AND SAIFULLAH SHAFIQ
Department of Electrical Engineering, King Fahd University of Petroleum and Minerals, Dhahran 31261, Saudi Arabia

Corresponding author: Umer Akram (g201512930@kfupm.edu.sa)

This work was supported by the Deanship of Research at the King Fahd University of Petroleum and Minerals under Project RG171009.

ABSTRACT Traditionally, the energy supply in off-grid communities has relied on diesel generating units based microgrids (MGs) but global environmental concerns and advancements in renewable energy technology are pushing for the transformation of these systems into renewable-based MGs. This transformation is a more complex hybrid system, with dispatchable and non-dispatchable resources, and requires novel planning and design tools to ensure the security of supply in the future. This paper presents a methodology that jointly optimizes the capacities and locations of dispatchable and non-dispatchable distributed generating units and battery energy storage system employed in a stand-alone MG serving conventional residential and electric vehicle charging load. The complex dual optimization problem is solved innovatively in two sequential steps. In the first step, the capacities of solar photovoltaic panels, wind turbines, battery energy storage system, and diesel generator are determined without actually considering the system design itself. While in the second step, a novel and simple methodology is developed which determines the sub-optimal capacities of distributed generation units along with their actual locations in the distribution system. To determine the optimal locations of distributed generation units, we defined a novel factor, losses-voltage-factor (LVF), which ensures reduced losses and better voltage quality. The proposed methodology gives a robust design that not only results in reduced losses and better voltage quality but also have higher reliability. The proposed technique is very practical, which can easily be applied for the planning and design of the practical active distribution networks.

INDEX TERMS Power system planning, renewable energy sources, battery energy storage, distributed generation, electrical vehicle.

I. INTRODUCTION

The electrical power system is transforming from centralized bulk system, with large-scale electric power generation system connected to the transmission network, to a decentralized system, with multiple small-scale electric power generating units connected directly to distribution system near the consumers. This type of small-scale generation is called distributed generation. The concept of distributed generation has evolved into idea of microgrid (MG), essentially a miniature version of the conventional grid [1]. Featuring distributed generators (DGs) and/or energy storage system, it embodies the capability to ''island'', isolate from the main grid, while operating parallel to it [2], [3]. Furthermore, for isolated and remote areas where supplying electricity through national grid is in-feasible due to techno-economic constraints, standalone MG is considered as a viable attractive alternative and thus adopted in many regions and countries [4]–[7]. The popularity of MGs is increasing, because they offer benefits in terms of renewable energy (RE) sources integration, greenhouse gases (GHG) emission reduction, power quality, reliability and resiliency, and economics [8], [9].

RE sources such as solar and wind are best suited for distributed generation because they are inexhaustible, non-polluting, and locally available [10]. The power output of RE sources technologies, i.e., solar photovoltaic (PV) panels and wind turbines (WTs) depends upon the natural resources, i.e., sun and wind which are stochastic, random, and intermittent as they depend upon climatic changes, weather, and time of the day and year. So, the output power of PV and WT may not follow the load which jeopardizes the reliability

2169-3536 © 2018 IEEE. Translations and content mining are permitted for academic research only.
Personal use is also permitted, but republication/redistribution requires IEEE permission.
See http://www.ieee.org/publications_standards/publications/rights/index.html for more information.

and power quality and can also cause voltage and frequency instability [11]–[13]. The special techno-economic challenges that arise due to integration of RE sources must be met for the stable and effective operation of system.

The problems associated with the RE sources can be addressed by storing energy during surplus generation hours by utilizing energy storage system and re-dispatching it appropriately afterwards when needed or by employing a diesel generator (DG) as a backup [14]–[19]. Several types of energy storage technologies are available and among them battery energy storage system (BESS) is most commonly utilized. The cost of BESS per kilowatt is strongly related to its capacity and it also has limited life cycles, therefore, supplying the demand at 100% reliability by using RE sources and BESS only may result in extremely high cost. Furthermore, the energy stored in BESS depends upon sporadic RE sources and during the operation of MG the output of RE sources and BESS can become inadequate to supply the load. Therefore, a dispatchable backup source, i.e., DG must be deployed along with PV, WT, and BESS to supply a load effectively and economically.

Transportation sector is one of the major contributors of the GHG emissions [20], [21]. The conventional vehicles use fossil fuels and emit GHG, i.e., carbon dioxide, nitrogen oxides, and carbon monoxide. Electric vehicles (EVs) have gained significant attention of both academia and industry since the last decade because of the escalating demand for fuel frugality and their eco-friendlier nature. Continuous improvements in EVs predict their vast penetration in the future electric power system, and the power demand diagram of the future grid would be conspicuously different from the present one without EVs [22], [23]. Therefore, significant number of EVs must be contemplated for future power system planning and design to ensure customers daily travel. So, the planning and design of future power system will not be alike the conventional power system, where all of the involved technologies should be considered at the planning and design stage.

In this paper, a technique for the planning and design of MG employing PV, WT, BESS, and DG is developed. The MG supplies conventional residential load and EV charging load. The planning and design problem is solved in two steps. In the first step, the capacity optimization of PV, WT, BESS, and DG is done without considering the dynamics of the test system. The capacity optimization is done on the basis of cost minimization and GHG emissions reduction. In the second step, the optimal locations of PV, WT, BESS, and DG and capacities for each location are determined. A very simple and practically implementable methodology, based upon the real power losses reduction and voltage quality, is developed to determine the optimal locations of distributed generation systems. Instead of installing distributed generation system at single location, the proposed methodology installs distributed generation units at multiple locations which results in better voltage quality, lesser losses, and robust system design. The proposed methodology is tested on real world 17 bus primary distribution system. Simulation results show that a system with distributed generation systems installed at multiple locations is more economical, robust, and stable as compared to single location. Simulation results also show that the proposed system design supplies the load economically and reliably.

The remainder of the paper is organized as follows. Section II discusses the literature review and research gap, Section III presents the proposed methodology. Results and Discussions are discussed in Section IV and Section V concludes the paper.

II. LITERATURE REVIEW AND RESEARCH GAP

In literature, different methodologies have proposed for the planning and design of MGs employing RE sources and energy storage technologies. The literature can be divided into two main classes. The first class discusses the capacity optimization of distributed generators and energy storage system. While the second class deals the location optimization and capacity and location optimization of distributed generators and energy storage system.

In the recent literature, considerable work has been done in the first class. In [24], a methodology for the capacity optimization of PV, WT, BESS, and super-capacitor has been proposed. The capacity optimization is done based upon the three objectives: 1) cost minimization, 2) reliability maximization, and 3) GHG emissions reduction. In [25], optimal capacities of PV, WT, DG, pumped storage, and BESS are determined based upon initial investment, operation, and maintenance costs minimization. In [26], sizing of PV, WT, BESS based MG is done on the basis of energy cost and reliability. In [27], a cost function, based upon the minimization of cost and maximization of customer satisfaction, is formulated for planning of grid-connected MG employing PV, WT, and BESS, and mixed integer linear programming is used to solve the optimization problem. In [28] a methodology has been developed for capacity optimization of a system employing PV, WT, and BESS. The proposed methodology is based upon the five key principles: i) higher reliability, ii) lesser fluctuations in the power sold to the main grid, ii) full use of the complementary attributes of wind and solar, iv) optimization of BESS charge-discharge rate, and v) minimization of total cost. In [29], sizing of PV and BESS is done on the basis of levelized cost of energy. In [30], optimal sizing of a residential MG employing PV, WT, and BESS is done based upon the cost minimization. In [31], a methodology has been proposed for the planning and design of residential small grid employing PV, WT, BESS and DG. The proposed technique is based upon the cost cost minimization, curtailment of GHG emissions, reduction of dump energy, and reliability maximization. In [32], the sizing of a standalone system employing PV, WT, BESS, and DG is done on the basis of three objectives, i.e., i) minimization of cost, ii) maximization of job creation, and iii) maximization of human development index. A pareto-optimization evolutionary algorithm is used to solve the optimization problem.

Similarly, some more techniques dealing with the planning and design of RE sources based MGs are discussed in [33]–[37].

In [38], a technique to determine the optimal size and location of WT is proposed. The technique is based upon the maximization of wind power generation. A novel chaotic symbiotic organisms search algorithm is used to determine the optimal sizes and location of distributed generators in radial distribution system. This distributed generators sizing and sitting problem is based upon minimization of real power losses and improvement of voltage stability [39]. A planning technique to determine the optimal sizes, locations and mix of conventional generators and RE sources is proposed in [40]. The proposed planning model considered investment, operation and maintenance, GHG emissions, and fuel costs. A methodology for sizing and location optimization of single PV distributed generator is developed in [41]. The methodology is based upon minimization of line losses, while keeping the voltage within permissible limits. In [42], backtracking search optimization algorithm is used to determine the optimal location of distributed generators. The location optimization is done based upon the the network real power loss reduction and enhancement of voltage profile. In [43], optimal size and location of distributed generator are found on the basis of minimizing power losses, operational cost minimization, and voltage stability improvement. Bacterial foraging optimization algorithm is used to find the optimal size of distributed generator. A methodology based upon annual energy losses minimization for the integration of conventional and renewable distributed generators is proposed in [44]. Ant Lion Optimization Algorithm is used for optimal sizing and location of distributed generators in a distribution system in [45]. The sizing and location optimization is done based upon the real power losses minimization and voltage profile improvement. Similarly, some more techniques dealing with the capacity and location optimization of RE sources are discussed in [46]–[49].

The literature deals with the capacity optimization of RE sources based MGs and location and sizing optimization of distributed generators. A new type of load, i.e., EV load, in future it would be major part of the power system load, is not considered properly for location and sizing optimization. Moreover, to the best knowledge of the authors no methodology has been developed so far that jointly determines the sizes and locations of multiple dispatchable and renewable distributed generators and energy storage system.

III. PROPOSED METHODOLOGY

Let $M = \{0, 1, \ldots, 11\}$ denotes number of months, $D = \{0, 1, \ldots, 29\}$ be the set containing number of days within a month, and $H = \{0, 1, \ldots, 23\}$ contains the hours number within a day. The indexing of a whole year is done by carrying cross product $(m, d, h) \in M \times D \times H$. The inter-month, inter-day, and inter-hour transitions follow $(m, d + 29, h) = (m + 1, 0, h)$, and $(m, d, h + 23) = (m, d + 1, 0)$ respectively.

TABLE 1. Characteristics of EVs.

EV Type	Battery bank (kWh)	Charg./Disch. rate (kW)	Maximum Mileage (mi)
Tesla S70	70	11	240
Nissan Leaf	24	6.6	126
Th!nk City	24	6.6	100

For the purpose of brevity the indexes $m, d,$ and h are removed and only index t will be used.

Let $\digamma^t = (P_L^t, P_R^t, P_B^t, S_B^t, P_D^t)$ be the state of the system at time t. S_B^t is the SOC of BESS at time t, P_B^t is power supplied or taken by of BESS in MW at time t, P_R^t is the power generated by PV and WT in MW at time t, P_D^t is the power output of DG in MW at time t, and P_L^t is the total load power demand in MW at any time t. The system states get updated after every one hour. In the next two subsections we will model the system states.

A. LOAD MODELING

The total load is sum of EV and non EV load, $P_L^t = P_{ev}^t + P_l^t$. In this study, three types of EVs are considered, i.e., Think City, Nissan Leaf, and Tesla S 70. The total number of EVs in the system are determined based upon the their penetration level in the system, $N_{ev} = \sum_{c=1}^{c_l} \rho v_c n_h$. ρ is the penetration level, v_c is the percentage of c^{th} class of EV, c_l is the total number of classes of EVs and n_h is the number of houses. The EV charging load depends upon the departure and arrival times, daily mileage traveled, charger rating of EV, and battery bank size. The charger rating and battery bank size can be obtained from manufacturer and given in Table 1. It is assumed that the EVs are charged at constant rate at their rated charging capacity. The departure and arrival times, daily mileage, and charging time depends upon the user behavior and can be approximated using lognormal distribution.

$$\kappa^{e,c,d} = logNormal(3.375, 0.5) \tag{1}$$

$$\overline{\tau}^{e,c,d} = logNormal(\Lambda_{dp}, \sqrt{3}) \tag{2}$$

$$\underline{\tau}^{e,c,d} = logNormal(\Lambda_{ar}, \sqrt{3}) \tag{3}$$

where $\kappa^{e,c,d}$ represents the total miles traveled by the e^{th} EV of c^{th} class at day d, $\overline{\tau}$ and $\underline{\tau}$ are departure and arrival times, and Λ_{dp} and Λ_{ar} are average departure and arrival times respectively. After determining the daily distance covered by an EV the energy required to charge it is calculated as follows

$$\hbar^{e,c,d} = E_{ev}^c \mathbf{1}_{(\kappa^{e,c,d} \geq \lambda^c)} + \frac{E_{ev}^c}{\lambda^c} \kappa^{e,c,d} \mathbf{1}_{(\kappa^{e,c,d} < \lambda^c)} \tag{4}$$

where $\mathbf{1}_{(\star)}$ is indicator function, $\hbar$ is total energy required to charge the EV, λ is charge depletion distance, and E_{ev} is the energy capacity of the EV's battery bank. The time required to fully charge the EV whose battery status is known is calculated using $\tau_{chg}^{e,c,d} = \hbar^{e,c,d} / p_{ev}^{e,c,d}$, τ_{chg} is time needed to charge an EV and p_{ev}^c is the charging rate of c^{th} class of EV. The charging rate of each EV must be within manufacturers'

specified limits, i.e., $0 \leq p_{ev}^{e,c,d} \leq p_{ev}^{c,max}$. It is assumed that the EVs owners will start charging their cars after arriving home. So, the charging load of EVs is determined as following

$$P_{chg}^{e,c,d}(\underline{\tau}^{e,c,d}+y) = p_{ev}^{c}\mathbf{1}_{\left(y\leq\tau_{chg}^{e,c,d}\right)} + p_{ev}^{c}\left(\tau_{chg}^{e,c,d}-\lfloor\tau_{chg}^{e,c,d}\rfloor\right)\mathbf{1}_{\left(y>\tau_{chg}^{e,c,d}\right)} \quad (5)$$

where

$$y = 1, 2, \ldots., \lfloor\tau_{chg}^{e,c,d}\rfloor + 1$$

and

$$\underline{\tau}^{e,c,d} + y > \overline{\tau}^{e,c,d}$$

where $P_{chg}^{e,c,d}$ is the hourly charging load of e^{th} EV of c^{th} class at day d. The index d in $P_{chg}^{e,c,d}$ can be replaced by t. The state-of-charge of battery bank of an EV at any time t is estimated as given below

$$SOC_{ev}^{e,c,t+\Delta t} = SOC_{ev}^{e,c,t} + \Delta t\frac{P_{chg}^{e,c,t}}{E_{ev}^{c}} \quad (6)$$

where SOC_{ev} is the state of charge of EV. At every time t the state-of-charge of battery bank of EV must remain within the permissible limits, i.e., $SOC_{ev}^{c,min} \leq SOC_{ev}^{e,c,t} \leq SOC_{ev}^{c,max}$. As, it is already mentioned that total load is sum of EV load and non-EV load. The non-EV load is taken from real world residential demand $\left(P_l^t\right)$ data with resolution of one hour. Due to confidentiality the exact location of residential load demand data is not declared.

B. DISTRIBUTED GENERATION SYSTEM MODELING

The distributed generation system consists of dispatchable source, i.e., DG, RE sources, i.e., PV and WT, and BESS. We are interested in determining the power output of DG, PV, and WT at any time t, and power supplied/taken and energy state of BESS at any time t.

The output power of RE sources is $P_R^t = N_{pv}P_{pv}^t + N_{wt}P_{wt}^t$, where N_{pv} is the number of PV panels, P_{pv}^t is the power output of one PV panel in MW at time t, N_{wt} is the number of WTs, P_{wt}^t is the power output of one WT in MW at time t. The number of PV panels and WTs are subjected to $N_{pv}^{min} \leq N_{pv} \leq N_{pv}^{max}$ and $N_{wt}^{min} \leq N_{wt} \leq N_{wt}^{max}$ respectively. The power output of single WT is calculated as in [50]

$$P_{wt}^t = \mathbf{1}_{(v_{ci}<v^t<v_r)}\varsigma(v^t) + \mathbf{1}_{(v_r\leq v^t<v_{co})}P_{wt}^r \quad (7)$$

where P_{wt}^r is the rated power of WT, $\varsigma(v)$ is the function that approximates the variation in wind power output with wind speed, v^t is wind speed at time t, v_{ci}, v_{co}, and v_r are cut-in, cut-out, and rated wind speeds of WT. The characteristics of GE 1.5xle WT (shown in Fig. 1) are used to model the power output of WT. The power output of PV system is estimated using following equation [51]

$$P_{pv}^t = \eta_{pv}A_{pv}I^t(1-0.0005(T_o^t-25)) \quad (8)$$

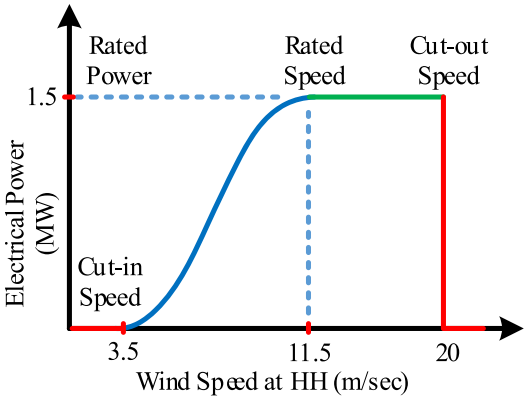

FIGURE 1. Power curve of GE 1.5xle WT.

where η_{pv} is efficiency of PV panel, I^t is solar irradiation at time t in MW/m^2, A_{pv} is area of PV panel in m^2, and T_o^t is atmospheric temperature in ^oC at time t. We define the difference between generation and demand as $x^t = P_R^t - P_L^t$. The power output of BESS is

$$P_B^t = \left[\mathbf{1}_{(0<x^t<P_B^{max})} + \mathbf{1}_{(-P_B^{max}<x^t<0)}\right]x^t + \left[\mathbf{1}_{(x^t>P_B^{max})} - \mathbf{1}_{(x^t<-P_B^{max})}\right]P_B^{max} \quad (9)$$

where P_B^{max} is the maximum power rating of BESS. A positive value of P_B represents charging and a negative value represents discharging of BESS. The BESS power constraint $P_B^{min} \leq |P_B^t| \leq P_B^{max}$ will always be satisfied by (9). The change in energy level of BESS is determined using equation given in [51]

$$S_B^t = S_B^{t-\Delta t} + P_B^t(\mathbf{1}_{(x^t>0)}\eta^c + \mathbf{1}_{(x^t<0)}\frac{1}{\eta^d})\Delta t \quad (10)$$

where η^c is charging efficiency and η^d is discharging efficiency. In (10) a positive value of P_B will result in an increase in energy level of BESS while a negative P_B will decrease in energy level of BESS. At every time t the energy level of BESS must remain within the permissible limits $S_B^{min} \leq S_B^t \leq S_B^{max}$. The BESS has limited number of life cycles. Therefore, for realistic analysis it is critical to calculate the cycles of BESS. The BESS annual life is estimated as following [52]

$$B_{cyc} = \sum_{m=0}^{11}\sum_{d=0}^{29}\sum_{h=0}^{23}\lfloor\frac{|P_B^{m,d,h}|}{2S_B^{max}}\rceil \quad (11)$$

where B_{cyc} are annual BESS cycles. In this study, we assume that after completing life cycles BESS must be replaced. Hence, the life of BESS in years is calculated as $T_B = \lfloor\frac{T_{cyc}}{B_{cyc}}\rceil$, T_{cyc} is the total number of life cycles and T_B is the life of BESS in years. As mentioned earlier, to improve the system reliability and economy a DG is also employed along with BESS. The DG serves as backup and supplies power only when power output of RE sources and BESS become inadequate to supply the load demand. The power output of DG is

calculated using the following mathematical expression

$$P_D^t = (P_B^t - x^t)\mathbf{1}_{(P_R^t - P_B^t < P_L^t)} \tag{12}$$

At every time t the DG must remain within its minimum and maximum allowable operational limits $P_D^{min} \leq P_D^t \leq P_D^{max}$. As both BESS and DG serves as backup, so it is crucial to develop an operation framework for them in which they supply the load demand while operating within their operational constraints. We define following two conditions and five rules

$$\begin{aligned}
&\mathbf{C1}: if\ P_D^t > P_B^{max} \quad then\ P_D^t = P_D^{max}\\
&\mathbf{C2}: if\ P_D^t < P_B^{min} \quad then\ P_D^t = P_D^{min}\\
&\mathbf{\Gamma_1}\ \mathcal{V}\ \ if\ x^{t+\Delta t} > 0 \quad and\ S_B^t + \Delta t P_B^{t+\Delta t} \leq S_B^{max}\ then\ P_D^{t+\Delta t}\\
&\qquad = \quad and\ S_B^{t+\Delta t} = S_B^t + P_B^t \Delta t \qquad (13)\\
&\mathbf{\Gamma_2}\ \mathcal{V}\ \ if\ x^{t+\Delta t} > 0 \quad and\ S_B^t + \Delta t P_B^{t+\Delta t} \geq S_B^{max}\ then\ P_D^{t+\Delta t}\\
&\qquad = 0 \quad and\ S_B^{t+\Delta t} = S_B^{max} \qquad (14)\\
&\mathbf{\Gamma_3}\ \mathcal{V}\ \ if\ x^{t+\Delta t} < 0 \quad and\ S_B^t + \Delta t P_B^{t+\Delta t} \geq S_B^{min}\ then\ P_D^{t+\Delta t}\\
&\qquad = P_B^{t+\Delta t} - x_{t+\Delta t} \quad and\ S_B^{t+\Delta t} = S_B^t + P_B^t \Delta t \qquad (15)\\
&\mathbf{\Gamma_4}\ \mathcal{V}\ \ if\ x^{t+\Delta t} < 0 \quad and\ S_B^t + \Delta t P_B^{t+\Delta t} < S_B^{min}\ then\ P_D^{t+\Delta t}\\
&\qquad = P_B^{t+\Delta t} - x_{t+\Delta t} \quad and\ S_B^{t+\Delta t} = S_B^{min} \qquad (16)\\
&\mathbf{\Gamma_5}\ \mathcal{V}\ \ if\ x^{t+\Delta t} = 0 \quad then\ P_D^{t+\Delta t} = 0\ and\ S_B^{t+\Delta t} = S_B^t \qquad (17)
\end{aligned}$$

The conditions **C1** and **C2** are necessary conditions for $\mathbf{\Gamma_i}\ \forall i = 1, 2, \ldots, 5$. Hence, $\mathbf{\Gamma_i} \Rightarrow \boldsymbol{C1}$ and $\mathbf{\Gamma_i} \Rightarrow \boldsymbol{C2}\ \ \forall i = 1, 2, \ldots, 5$. It is important to note that the BESS power and energy constraints will always be satisfied.

C. PROBLEM FORMULATION

Cost plays a key role in every engineering design. In this study, for realistic analysis we have assumed initial investment cost, operation cost, maintenance cost, and replacement cost.

We define $C_T = \sum (C_R, C_B, C_D)$ be the system's total cost. C_R is the initial investment, operation, and maintenance cost of RE sources, C_B is the initial investment, replacement, operation, and maintenance costs of BESS, and C_D incorporates the initial investment, replacement, operation, and maintenance costs of DG. The cost of RE sources is calculated as following

$$C_R = C_{pv}^c N_{pv} P_{pv}^r + C_{wt}^c N_{wt} P_{wt}^r + \sum_{l=1}^{n_l} \frac{C_{pv}^{om} N_{pv} P_{pv}^r + C_{wt}^{om} N_{wt} P_{wt}^r}{(1+d)^{l-1}} \tag{18}$$

where C_{pv}^c is the initial investment cost of PV in $\$/MW$, C_{wt}^c is the initial investment cost of WT in $\$/MW$, C_{pv}^{om} is operation and maintenance cost of PV in $\$/MW/yr$, C_{wt}^{om} is operation and maintenance cost of WT in $\$/MW/yr$, l is the year index, n_l is the years of operation, and d is the discount rate. The total cost of BESS depends upon the energy and power capacity of BESS and modeled as given below

$$C_B = C_B^e S_B^{max} + C_B^p P_B^{max} + \sum_{l=1}^{n_l} \frac{C_B^{om}}{(1+d)^{l-1}} + \sum_{l_B}^{n_l - T_B} \frac{C_B^e S_B^{max} + C_B^p P_B^{max}}{(1+d)^{l_B}} \tag{19}$$

where

$$l_B = T_B, 2T_B, \ldots, n_l - T_B$$

where C_B^e is the initial investment cost in $\$/MWh$ associated with energy capacity of BESS, C_B^p is the initial investment cost in $\$/MW$ associated with power capacity of BESS, C_B^{om} is the operation and maintenance cost in $\$/MW/yr$, and the third term in (19) constitutes for the replacement cost of BESS. The cost associated with the diesel generation system is modeled as following

$$C_D = \sum_{i=1}^{n_{dg}} C_{dg}^{c,i} P_{dg}^{r,i} + \sum_{i=1}^{n_d} \sum_{s=\ell_{dg}^i}^{n_l - \ell_{dg}^i} \frac{1}{(1+d)^s} C_{dg}^{c,i} P_{dg}^{r,i} + \sum_{i=1}^{n_{dg}} \sum_{j=1}^{n_l} \sum_{t=1}^{n} \frac{N_{run}^i M_{dg}^i}{(1+d)^{j-1}} \left(\Psi^i p_{dg}^{i,t} + \varphi^i P_{dg}^{r,i}\right) f_p \tag{20}$$

where

$$s = \ell_{dg}^i, 2\ell_{dg}^i, 3\ell_{dg}^i, \ldots . n_l - \ell_{dg}^i$$

where $C_{dg}^{c,i}$ is investment cost of i^{th} DG (in this study, to make system economical and efficient we have assumed multiple small DGs instead of considering one single large DG) in $\$/MW$, $P_{dg}^{r,i}$ is the rated capacity of i^{th} DG in MW, n_{dg} is the total number of DGs, ℓ^i is the life of i^{th} DG, N_{run}^i is the total operation time of i^{th} DG in hr, M_{dg}^i is the operation and maintenance cost of i^{th} DG in $\$/hr$, f_p is the fuel price in $\$/ltr$, P_{dg}^i is the power output of i^{th} DG, Ψ^i is the fuel curve slope coefficient of i^{th} DG, and φ^i is the fuel curve intercept coefficient of i^{th} DG. In (20), the first term represent the initial investment cost of diesel generation system, second term stands for the replacement cost, third term stands for the present worth of the cost associated with the operation and maintenance costs and fuel cost of diesel generation system.

As discussed earlier that one major advantage of RE sources is the reduction of GHG emissions. In this study, we modeled the GHG emissions in terms of cost. When electric energy is generated using conventional generators it results in GHG emissions and a correction cost is required to mitigate the damage caused by them tabulated in Table 2. This correction cost would be a saving if RE sources are employed for generation instead of fossil fuel based generators. This saving is termed as emission reduction benefit cost (ERBC) and calculated using the following equation

$$C_{erbc} = \sum_{j=1}^{n_l} \sum_{r=1}^{4} \sum_{t=1}^{n} \frac{\left[(P_R^t - P_B^t)\,\mathbf{1}_{(x^t<0)} + P_R^t \mathbf{1}_{(x^t \geq 0)}\right]}{(1+d)^{j-1}} E^r E_c^r \tag{21}$$

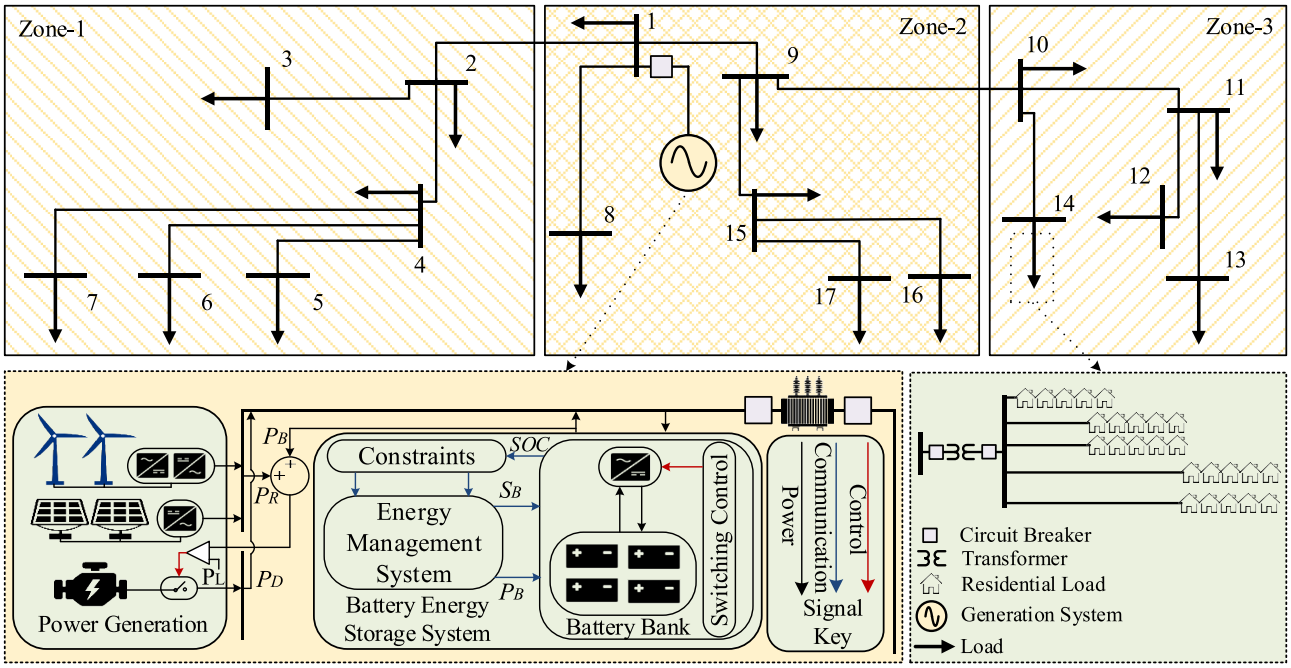

FIGURE 2. Primary distribution system.

TABLE 2. Greenhouse gases emission data.

Greenhouse gases	CO_2	CO	SO_2	NOx
Emissions (kg/MWh)	1000.7	1.55	9.993	6.46
Correction Cost ($/kg)	0.0037	0.16	0.97	1.29

where C_{erbc} is ERBC in \$, E^r is the emission of r^{th} type of GHG gas in kg/MW, and E_c^r is the correction cost of r^{th} type of greenhouse gas in $\$/kg$.

We propose the following objective function for the minimization of life cycle cost and GHG emissions.

$$obj: \; J = \sqrt{(J_1(\boldsymbol{X}) - J_2(\boldsymbol{X}))^2} \rightarrow \min \tag{22}$$

$$s.t. \begin{cases} \boldsymbol{g}_\ell(\boldsymbol{X}) = 0 & \ell = 1, 2, , \ldots, m \\ \boldsymbol{h}_\iota(\boldsymbol{X}) \leq 0 & \iota = 1, 2, , \ldots, q \end{cases} \tag{23}$$

where

$$\boldsymbol{X} = \left[N_{pv},\ N_{wt},\ E_B^{max},\ P_B^{max},\ P_D^{max}\right] \tag{24}$$

where $J_1(\boldsymbol{X})$ is the total cost of system which is the sum of cost of RE sources (18), cost of BESS (19), and cost of diesel generation system (20), $J_2(\boldsymbol{X})$ represents the GHG emissions, which are modeled in terms of ERBC (21), $\boldsymbol{g}_\ell$ represents the equality constraints, and $\boldsymbol{h}_\iota$ represents the inequality constraints. The system constraints are listed below:

The Primary System Constraint (Generation = Demand):

$$P_R^t + P_B^t + P_D^t - P_L^t = 0 \quad \forall t > 0 \tag{25}$$

The renewable generation system constraints:

$$N_{pv}^{min} \leq N_{pv} \leq N_{pv}^{max} \tag{26}$$

$$N_{wt}^{min} \leq N_{wt} \leq N_{wt}^{max} \tag{27}$$

BESS constraints:

$$P_B^{min} \leq |P_B^t| \leq P_B^{max} \quad \forall t > 0 \tag{28}$$

$$S_B^{min} \leq S_B^t \leq S_B^{max} \quad \forall t > 0 \tag{29}$$

Diesel generation system constraints:

$$P_D^{min} \leq P_D^t \leq P_D^{max} \tag{30}$$

EV load constraints:

$$SOC_{ev}^{c,min} \leq SOC_{ev}^{e,c,t} \leq SOC_{ev}^{c,max} \quad \forall e, c, t > 0 \tag{31}$$

$$0 \leq p_{ev}^{e,c,t} \leq p_{ev}^{c,max} \quad \forall e, c, t > 0 \tag{32}$$

The system is operated using the rules and an efficient metaheauristic technique, i.e., Teaching Learning Based Optimization, i.e., TLBO is used to solve optimization problem formulated in (22).

Consider 17-bus distribution system shown in Fig 2. We divide the distribution system in three zones, i.e., Zone-1, Zone-2, and Zone-3 and each zone is treated as independent MG. In order to determine the optimal location of generation system we define the following factor for each zone.

$$l_f^i = \sum_{j=1, j\neq i}^{n_{bus}} \boldsymbol{P_l}^j \cdot \boldsymbol{\ell}^j \quad \forall i = 1, 2, \ldots, n_{bus} \tag{33}$$

where l_f^i is the Losses-Voltage Factor (LVF) when generation system is placed at i, $\boldsymbol{P_l}^j$ is the vector of power which flows

TABLE 3. Optimal capacities of different MG topologies.

PV (MW)	WT (MW)	BESS (MWh)	BESS (MW)	DG (MW)	Cost (c/kWh)	Renewable Energy Served (GWh)	Non-Renewable Energy Served (GWh)
10	4	16.8	2.5	4	26.6	19.9	4.55

from bus j, and $\boldsymbol{\ell}^j$ is a vector whose elements are length of line that is connected to j and its order is $1 \times \left(ColumnsOf\, \boldsymbol{P_l}^j\right)$. For example, if generation system is placed at bus-2 then $l_f^2 = \left[P_l^3\right] \cdot [l_3] + \left[P_l^4\ P_l^5\ P_l^6\ P_l^7\right] \cdot [l_4\ l_4\ l_4\ l_4] + \left[P_l^5\ P_l^6\ P_l^7\right] \cdot [l_5\ l_5\ l_5] + \left[P_l^6\right] \cdot [l_6] + \left[P_l^7\right] \cdot [l_7]$. We define a vector, $\boldsymbol{L_f} = \left[l_f^1\ l_f^2\ \ldots\ l_f^{n_{bus}}\right]$, that contains the values of l_f of all buses. The optimal location corresponds to the bus number for which the value of l_f is minimum. The power generation share that is employed in each zone is determined using following

$$\boldsymbol{X}^z = \frac{\sum_{i=1}^{n_{bus}^z} P_l^i}{\sum_{i=1}^{n_{bus}} P_l^i} \boldsymbol{X} \tag{34}$$

where z is the zone number, n_{bus} is total number of buses in the distribution system, n_{bus}^z is the number of buses in zone number z, $\boldsymbol{X}$ is the vector that contains optimal capacities of PV, WT, BESS, and DG determined for whole system, and $\boldsymbol{X}^z$ is a vector that contains the optimal capacities of distributed generation resources that are employed in z^{th} zone.

IV. RESULTS AND DISCUSSIONS

The first step of the proposed methodology is to determine the optimal capacities of PV, WT, BESS, and DG that supply the load at lower cost and reduced GHG emissions. The cost function formulated in (22) is solved using TLBO. The variation in global best with the number of iterations is shown in Fig. 3. It can be observed that TLBO reaches optimal solution quickly. The optimal capacities that correspond to the optimal solution are tabulated in Table 3. As BESS is characterized by its power (MW) and energy (MWh) capacities that is why both power and energy capacities of BESS are given. The system serves around 80% of the total energy demand using RE sources.

The load power demand, power generated by RE sources, power output of BESS, and power output of DG for 24 hours are shown in Fig. 4, and the variation in energy level of BESS for the 24 hours is shown in Fig. 5. During the first two hours the output power of RE sources is zero and load is supplied by BESS and DG. The negative values of BESS output means BESS is supplying power. At the end of second hour the power output of BESS becomes zero because battery is discharged completely. It can be observed from the Fig. 4 that DG is used as backup which supplies load only when output of RE sources and BESS becomes insufficient to supply the load. Moreover, the BESS operates within its power and energy constraints. For example, from hour 12 to 16 the excessive power is available but BESS takes the amount of power that is within its maximum MW rating,

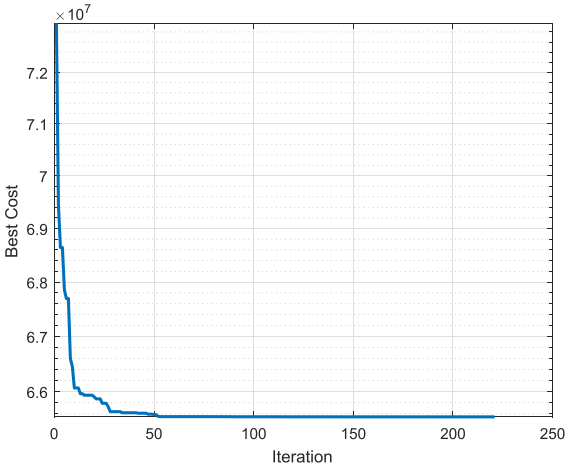

FIGURE 3. Global best vs iteration number.

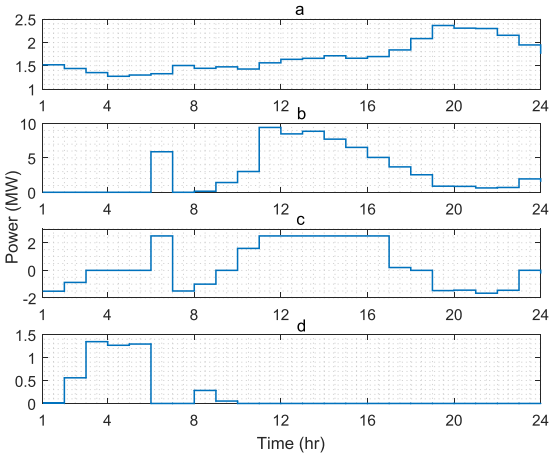

FIGURE 4. Variation in power. (a) Load power demand (b) Power generated by RE sources, (c) Power output of BESS, (d) Power output of DG.

i.e, 2.5 MW. After reaching the maximum energy capacity level, i.e., 16.6 MWh BESS stops charging and the excessive power is dumped.

The second step is the determination of optimal locations of distributed generation systems such that system has reduced line losses and better voltage quality. The distributed generation system is composed of PV, WT, BESS, and DG coupled system. As discussed earlier, the distribution system is divided into three zones (Zone-1, Zone-2, and Zone-3) and optimal location for distributed generation system for each zone is determined independently. The capacity of distributed generation systems for each zone are determined as given in (34). To determine the optimal locations the values of

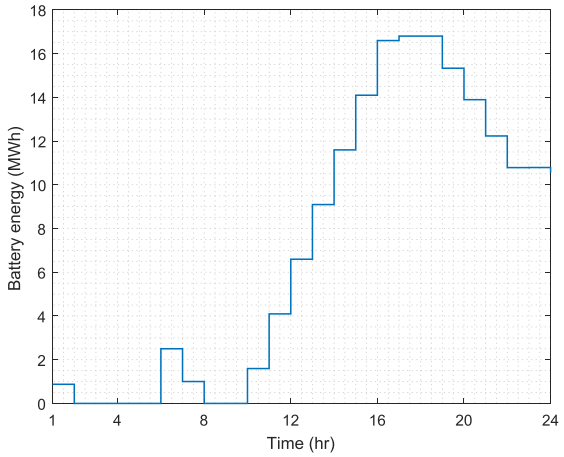

FIGURE 5. Variation in energy level of BESS.

LVF (33) are calculated for each bus of the three zones and shown in Fig. 6a. In Zone-1 the LVF is minimum for bus number 4 and maximum for bus number 7. Hence, for Zone-1 the optimal location for the placement of distributed generation system in bus number 4 and worst location is bus number 7. Similarly, in Zone-2 the minimum value of LVF is for bus number 15 and bus number 9 while maximum LVF corresponds to bus number 8. Therefore, in Zone-2 the best location for the deployment of distributed generation system is bus 9 or bus 15 and worst location is bus number 8. Similarly, the best and worst locations in Zone-3 are bus number 11 and bus number 12 respectively.

To validate the proposed technique the distributed generation systems are placed at the optimal locations and system is operated and voltages at all the buses are calculated and shown in Fig. 6b. The upper limit of non-critical voltage window is considered as 1.05 pu and lower limit of non-critical voltage window is assumed as 0.95 pu. It can be observed that all bus voltages are above 0.98 pu. To show the effectiveness of the proposed methodology the distributed generators are also placed at the worst locations of Zone-1, Zone-2, and Zone-3. The bus voltages that correspond to the worst locations are shown in Fig. 6c. It can be observed that the voltages for the worst locations of distributed generation systems are scattered and voltage of bus 16 and 17 are at the lower limit of non-critical voltage window. Therefore, it can be deduced from Fig. 6b and Fig. 6c that the quality of voltage for optimal locations is better. Moreover, line losses for best and worst locations are calculated and compared. The line losses for worst locations are 2.7 times the losses for optimal location. So placing the generation system at optimal location can result in considerable savings. The above discussion proves that the smaller value of LVF ensures better voltage quality and reduced system losses.

The optimal location of distributed generation system is also determined without dividing the distribution system in different zones. The value of LVF is calculated for each bus and shown in Fig. 7a. It can be observed that LVF value is minimum for bus number 9 and maximum for bus number 7.

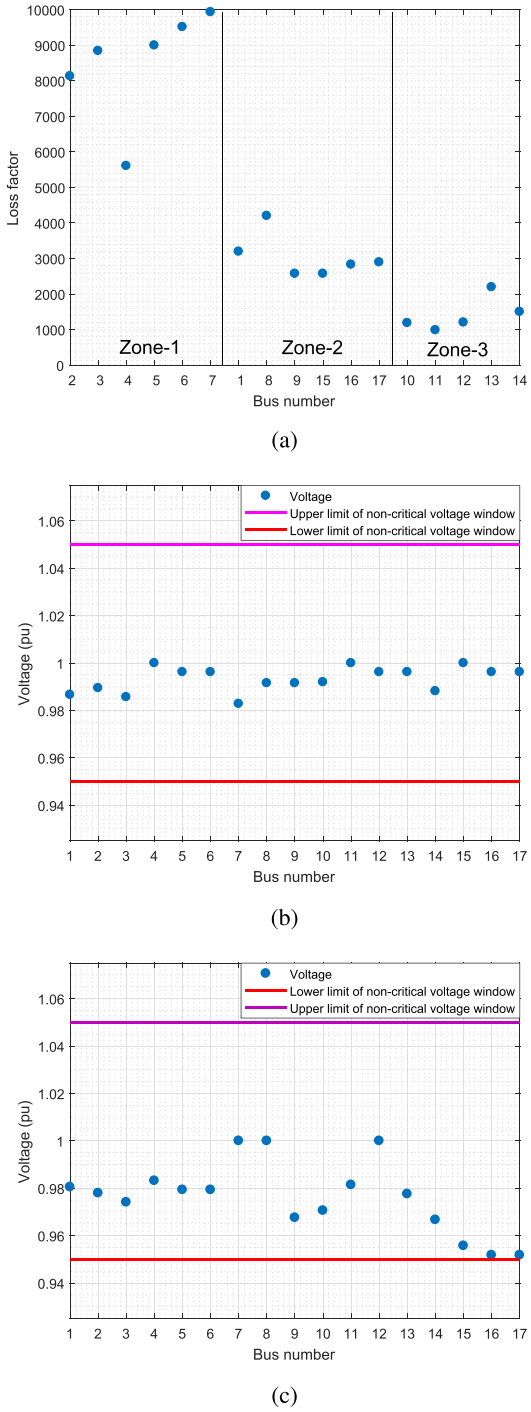

FIGURE 6. (a) LVFs for multiple distributed generating units. (b) Bus voltages corresponding to optimal locations of multiple distributed generation units. (c) Bus voltages corresponding to worst locations of multiple distributed generation units.

Hence, for single point distributed generation system feeding the optimal and worst locations are bus number 9 and bus number 7 respectively. The bus voltages when the system is fed from bus number 9, i.e., optimal location, are shown in Fig. 7b. It can be observed that the voltage at buses 2-6 are below the non-critical voltage window which is unacceptable. Similarly, the distributed generators are placed at

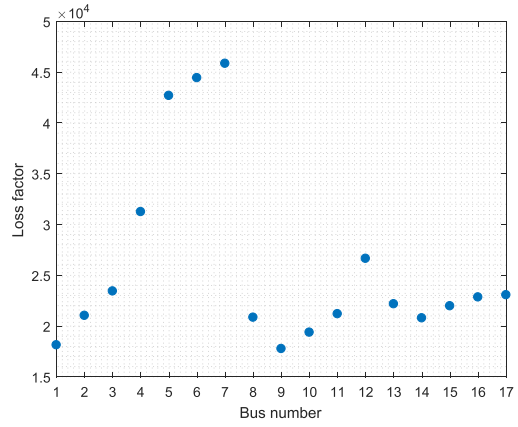

(a)

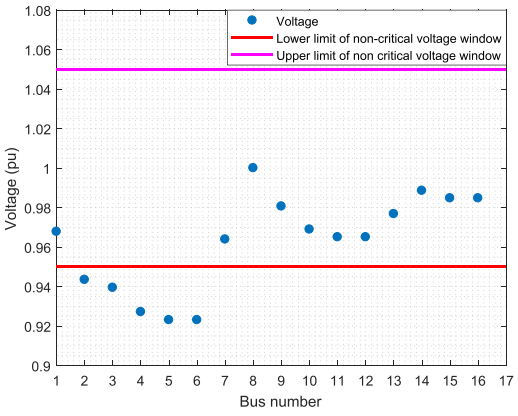

(b)

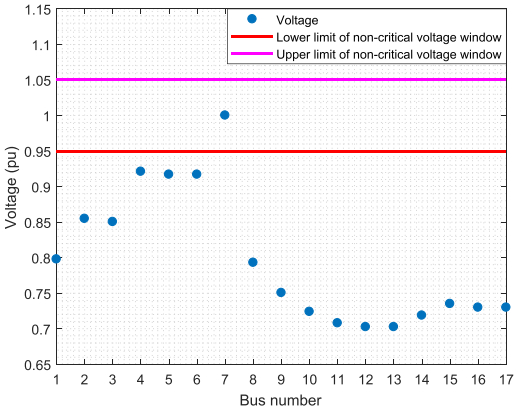

(c)

FIGURE 7. (a) LVFs for single location. (b) Bus voltages corresponding to optimal locations of multiple distributed generation units. (c) Bus voltages corresponding to worst location of single distributed generation system.

worst location, i.e., bus number 7, and bus voltages are determined and shown in Fig. 7c. It can be observed that except the generation bus, all bus voltages are below the lower limit of non-critical voltage window. Line losses for best and worst locations are calculated and the line losses for worst case are 6.35 times of the optimal location.

Line losses for single point distributed generation system feeding at optimal location are 3.36 times more than that of multiple point distributed generation systems feeding at the optimal locations. It can also be observed from the Fig. 6a and Fig. 7a that value of LVF for multiple distributed generation systems typology are significantly less than that of single generation system topology. Due to this reason the voltages for single generation system are of very poor quality as compared to multiple generators topology Fig. 7b and Fig. 6b. Moreover, the system with multiple generation facilities is more robust and reliable as compared to single generation facility. In case of outage of a line in any zone some portion of load of defected zone can be supplied by supplying power from the neighboring zones. In addition, preventive maintenance of the generation facilities can be performed with lesser load shedding with multiple distributed generation systems topology. Hence, the proposed methodology provides a solution which serves load with green energy, at better voltage quality, reduced system losses, reduced GHG emissions, and higher system reliability.

V. CONCLUSION

In this paper, capacity and location optimization of multiple distributed generating units in a standalone MG system are jointly determined based on dual optimization concept particularly considering EV charging load in addition to a typical conventional residential load. The mathematical models of all given generating units like PV, WT, BESS, DG, and EV-load have also been formulated. The primary optimization determines the optimal sizes of distributed generators and energy storage system based upon minimization of cost and GHG emissions. A relatively simple and more realistic suboptimization algorithm has been developed that determines the optimal locations of distributed generators consequently based on the voltage quality improvement and real power losses reduction. The proposed methodology has been tested on a real-world 17-bus primary distribution system. It has been observed that the proposed multiple objective design fulfills the power demand with a very good voltage quality and reduced losses. Furthermore, a comparison has been made for a single optimal location system and proposed multiple optimal locations system in terms of real power losses and voltage profiles to justify that the proposed scheme supplies load with reduced losses and better power quality.

ACKNOWLEDGMENT

The authors would like to thank Research Institute (RI) at KFUPM and Saudi Electricity Company (SEC) for providing renewables and demand data to carry out this research. This work was supported by the Deanship of Research at the King Fahd University of Petroleum and Minerals under Project RG171009.

REFERENCES

[1] C. D. Korkas, S. Baldi, I. Michailidis, and E. B. Kosmatopoulos, "Occupancy-based demand response and thermal comfort optimization in microgrids with renewable energy sources and energy storage," *Appl. Energy*, vol. 163, pp. 93–104, Feb. 2016.

[2] M. A. Allam, A. A. Hamad, M. Kazerani, and E. F. El Saadany, "A novel dynamic power routing scheme to maximize loadability of islanded hybrid AC/DC microgrids under unbalanced AC loading," *IEEE Trans. Smart Grid*, to be published, doi: 10.1109/TSG.2017.2697360.

[3] T. John and S. P. Lam, "Voltage and frequency control during microgrid islanding in a multi-area multi-microgrid system," *IET Gener., Transmiss. Distrib.*, vol. 11, no. 6, pp. 1502–1512, Apr. 2017.

[4] M. Marzband, E. Yousefnejad, A. Sumper, and J. L. Domínguez-García, "Real time experimental implementation of optimum energy management system in standalone microgrid by using multi-layer ant colony optimization," *Int. J. Elect. Power Energy Syst.*, vol. 75, pp. 265–274, Feb. 2016.

[5] T. Ma, H. Yang, and L. Lu, "A feasibility study of a stand-alone hybrid solar–wind–battery system for a remote island," *Appl. Energy*, vol. 121, pp. 149–158, May 2014.

[6] T. Ma, H. Yang, L. Lu, and J. Peng, "Technical feasibility study on a standalone hybrid solar-wind system with pumped hydro storage for a remote island in Hong Kong," *Renew. Energy*, vol. 69, pp. 7–15, Sep. 2014.

[7] Y. Kuang *et al.*, "A review of renewable energy utilization in islands," *Renew. Sustain. Energy Rev.*, vol. 59, pp. 504–513, Jun. 2016.

[8] S. Mashayekh, M. Stadler, G. Cardoso, and M. Heleno, "A mixed integer linear programming approach for optimal DER portfolio, sizing, and placement in multi-energy microgrids," *Appl. Energy*, vol. 187, pp. 154–168, Feb. 2017.

[9] L. Che, X. Zhang, M. Shahidehpour, A. Alabdulwahab, and A. Abusorrah, "Optimal interconnection planning of community microgrids with renewable energy sources," *IEEE Trans. Smart Grid*, vol. 8, no. 3, pp. 1054–1063, May 2017.

[10] J. Twidell and T. Weir, *Renewable Energy Resources*. Evanston, IL, USA: Routledge, 2015.

[11] A. Khatamianfar, M. Khalid, A. V. Savkin, and V. G. Agelidis, "Improving wind farm dispatch in the australian electricity market with battery energy storage using model predictive control," *IEEE Trans. Sustain. Energy*, vol. 4, no. 3, pp. 745–755, Jul. 2013.

[12] M. Khalid, A. Ahmadi, A. V. Savkin, and V. G. Agelidis, "Minimizing the energy cost for microgrids integrated with renewable energy resources and conventional generation using controlled battery energy storage," *Renew. Energy*, vol. 97, pp. 646–655, Nov. 2016.

[13] U. Akram and M. Khalid, "A coordinated frequency regulation framework based on hybrid battery-ultracapacitor energy storage technologies," *IEEE Access*, vol. 6, pp. 7310–7320, 2018.

[14] D. Parra, S. A. Norman, G. S. Walker, and M. Gillott, "Optimum community energy storage for renewable energy and demand load management," *Appl. Energy*, vol. 200, pp. 358–369, Aug. 2017.

[15] R. K. Sharma and S. Mishra, "Dynamic power management and control of a PV PEM fuel-cell-based standalone AC/DC microgrid using hybrid energy storage," *IEEE Trans. Ind. Appl.*, vol. 54, no. 1, pp. 526–538, Jan./Feb. 2018.

[16] A. V. Savkin, M. Khalid, and V. G. Agelidis, "A constrained monotonic charging/discharging strategy for optimal capacity of battery energy storage supporting wind farms," *IEEE Trans. Sustain. Energy*, vol. 7, no. 3, pp. 1224–1231, Jul. 2016.

[17] T. R. Oliveira, W. W. A. G. Silva, and P. F. Donoso-Garcia, "Distributed secondary level control for energy storage management in DC microgrids," *IEEE Trans. Smart Grid*, vol. 8, no. 6, pp. 2597–2607, Nov. 2017.

[18] K. Kant, C. Jain, and B. Singh, "A hybrid diesel-wind-PV-based energy generation system with brushless generators," *IEEE Trans. Ind. Informat.*, vol. 13, no. 4, pp. 1714–1722, Aug. 2017.

[19] M. Khalid and A. V. Savkin, "A model predictive control approach to the problem of wind power smoothing with controlled battery storage," *Renew. Energy*, vol. 35, no. 7, pp. 1520–1526, 2010.

[20] S. C. Davis, *Transportation Energy Data Book*, 22nd ed. Collingdale, PA, USA: DIANE, 2002.

[21] S. Shafiq, M. A. Aslam, M. Khalid, A. Raza, and U. Akram, "Implementation of electric drive system using induction motor for traction applications," in *Proc. IEEE 6th Int. Conf. Clean Electr. Power (ICCEP)*, Jun. 2017, pp. 673–677.

[22] A. Y. Saber and G. K. Venayagamoorthy, "Resource scheduling under uncertainty in a smart grid with renewables and plug-in vehicles," *IEEE Syst. J.*, vol. 6, no. 1, pp. 103–109, Mar. 2012.

[23] T. Sousa, H. Morais, Z. Vale, P. Faria, and J. Soares, "Intelligent energy resource management considering vehicle-to-grid: A simulated annealing approach," *IEEE Trans. Smart Grid*, vol. 3, no. 1, pp. 535–542, Mar. 2012.

[24] U. Akram, M. Khalid, and S. Shafiq, "An innovative hybrid wind-solar and battery–supercapacitor microgrid system—Development and optimization," *IEEE Access*, vol. 5, pp. 25897–25912, 2017.

[25] P. Yang and A. Nehorai, "Joint optimization of hybrid energy storage and generation capacity with renewable energy," *IEEE Trans. Smart Grid*, vol. 5, no. 4, pp. 1566–1574, Jul. 2014.

[26] U. Akram, M. Khalid, and S. Shafiq, "Optimal sizing of a wind/solar/battery hybrid grid-connected microgrid system," *IET Renew. Power Gener.*, vol. 12, no. 1, pp. 72–80, Jan. 2018.

[27] J. Chen *et al.*, "Optimal sizing for grid-tied microgrids with consideration of joint optimization of planning and operation," *IEEE Trans. Sustain. Energy*, vol. 9, no. 1, pp. 237–248, Jan. 2018.

[28] L. Xu, X. Ruan, C. Mao, B. Zhang, and Y. Luo, "An improved optimal sizing method for wind-solar-battery hybrid power system," *IEEE Trans. Sustain. Energy*, vol. 4, no. 3, pp. 774–785, Jul. 2013.

[29] C. S. Lai and M. D. McCulloch, "Sizing of stand-alone solar PV and storage system with anaerobic digestion biogas power plants," *IEEE Trans. Ind. Electron.*, vol. 64, no. 3, pp. 2112–2121, Mar. 2017.

[30] R. Atia and N. Yamada, "Sizing and analysis of renewable energy and battery systems in residential microgrids," *IEEE Trans. Smart Grid*, vol. 7, no. 3, pp. 1204–1213, May 2016.

[31] U. Akram, M. Khalid, and S. Shafiq, "An improved optimal sizing methodology for future autonomous residential smart power systems," *IEEE Access*, vol. 6, pp. 5986–6000, 2018.

[32] R. Dufo-López, I. R. Cristóbal-Monreal, and J. M. Yusta, "Optimisation of PV-wind-diesel-battery stand-alone systems to minimise cost and maximise human development index and job creation," *Renew. Energy*, vol. 94, pp. 280–293, Aug. 2016.

[33] H. Lotfi and A. Khodaei, "Hybrid AC/DC microgrid planning," *Energy*, vol. 118, pp. 37–46, Jan. 2017.

[34] E. E. Sfikas, Y. A. Katsigiannis, and P. S. Georgilakis, "Simultaneous capacity optimization of distributed generation and storage in medium voltage microgrids," *Int. J. Elect. Power Energy Syst.*, vol. 67, pp. 101–113, May 2015.

[35] V. Kalkhambkar, R. Kumar, and R. Bhakar, "Joint optimal allocation methodology for renewable distributed generation and energy storage for economic benefits," *IET Renew. Power Gener.*, vol. 10, no. 9, pp. 1422–1429, Oct. 2016.

[36] L. Che, X. Zhang, M. Shahidehpour, A. Alabdulwahab, and Y. Al-Turki, "Optimal planning of loop-based microgrid topology," *IEEE Trans. Smart Grid*, vol. 8, no. 4, pp. 1771–1781, Jul. 2017.

[37] F. S. Gazijahani and J. Salehi, "Stochastic multi-objective framework for optimal dynamic planning of interconnected microgrids," *IET Renew. Power Gener.*, vol. 11, no. 14, pp. 1749–1759, Dec. 2017.

[38] H. Cetinay, F. A. Kuipers, and A. N. Guven, "Optimal siting and sizing of wind farms," *Renew. Energy*, vol. 101, pp. 51–58, Feb. 2017.

[39] S. Saha and V. Mukherjee, "Optimal placement and sizing of DGs in RDS using chaos embedded SOS algorithm," *IET Gener., Transmiss. Distrib.*, vol. 10, no. 14, pp. 3671–3680, Nov. 2016.

[40] Z. Wang, B. Chen, J. Wang, J. Kim, and M. M. Begovic, "Robust optimization based optimal DG placement in microgrids," *IEEE Trans. Smart Grid*, vol. 5, no. 5, pp. 2173–2182, Sep. 2014.

[41] A. Al-Sabounchi, J. Gow, and M. Al-Akaidi, "Simple procedure for optimal sizing and location of a single photovoltaic generator on radial distribution feeder," *IET Renew. Power Gener.*, vol. 8, no. 2, pp. 160–170, Mar. 2014.

[42] A. El-Fergany, "Optimal allocation of multi-type distributed generators using backtracking search optimization algorithm," *Int. J. Elect. Power Energy Syst.*, vol. 64, pp. 1197–1205, Jan. 2015.

[43] A. M. Imran and M. Kowsalya, "Optimal size and siting of multiple distributed generators in distribution system using bacterial foraging optimization," *Swarm Evol. Comput.*, vol. 15, pp. 58–65, Apr. 2014.

[44] D. Q. Hung, N. Mithulananthan, and K. Y. Lee, "Optimal placement of dispatchable and nondispatchable renewable DG units in distribution networks for minimizing energy loss," *Int. J. Elect. Power Energy Syst.*, vol. 55, pp. 179–186, Feb. 2014.

[45] E. S. Ali, S. M. A. Elazim, and A. Y. Abdelaziz, "Ant lion optimization algorithm for optimal location and sizing of renewable distributed generations," *Renew. Energy*, vol. 101, pp. 1311–1324, Feb. 2017.

[46] G. Muñoz-Delgado, J. Contreras, and J. M. Arroyo, "Joint expansion planning of distributed generation and distribution networks," *IEEE Trans. Power Syst.*, vol. 30, no. 5, pp. 2579–2590, Sep. 2015.

[47] D. Q. Hung and N. Mithulananthan, "Multiple distributed generator placement in primary distribution networks for loss reduction," *IEEE Trans. Ind. Electron.*, vol. 60, no. 4, pp. 1700–1708, Apr. 2013.
[48] S. Devi and M. Geethanjali, "Application of modified bacterial foraging optimization algorithm for optimal placement and sizing of distributed generation," *Expert Syst. Appl.*, vol. 41, no. 6, pp. 2772–2781, 2014.
[49] A. Ahmadian, M. Sedghi, A. Elkamel, M. Aliakbar-Golkar, and M. Fowler, "Optimal WDG planning in active distribution networks based on possibilistic–probabilistic PEVs load modelling," *IET Generat., Transmiss. Distrib.*, vol. 11, no. 4, pp. 865–875, Mar. 2017.
[50] A. Arabali, M. Ghofrani, M. Etezadi-Amoli, and M. S. Fadali, "Stochastic performance assessment and sizing for a hybrid power system of solar/wind/energy storage," *IEEE Trans. Sustain. Energy*, vol. 5, no. 2, pp. 363–371, Apr. 2014.
[51] S. X. Chen, H. B. Gooi, and M. Q. Wang, "Sizing of energy storage for microgrids," *IEEE Trans. Smart Grid*, vol. 3, no. 1, pp. 142–151, Mar. 2012.
[52] G. He, Q. Chen, C. Kang, Q. Xia, and K. Poolla, "Cooperation of wind power and battery storage to provide frequency regulation in power markets," *IEEE Trans. Power Syst.*, vol. 32, no. 5, pp. 3559–3568, Sep. 2017.

MUHAMMAD KHALID received the Ph.D. degree in electrical engineering from the School of Electrical Engineering & Telecommunications (EE&T), University of New South Wales (UNSW), Sydney, Australia, in 2011. He was a Post-Doctoral Research Fellow School of EE&T, UNSW, for three years, where he then continued as a Senior Research Associate with the Australian Energy Research Institute for another two years. He is currently serving as an Assistant Professor with the Electrical Engineering Department, King Fahd University of Petroleum and Minerals, Dhahran, Saudi Arabia. His current research interests include the optimization and control of battery energy storage systems for large-scale grid-connected renewable power plants (particularly wind and solar), distributed power generation and dispatch, hybrid energy storage, EVs, and smart grids. He has authored/co-authored several journal and conference papers in the field of control and optimization for renewable power systems. In addition, he has been a Reviewer for numerous international journals and conferences. He was a recipient of a highly competitive post-doctoral writing fellowship from UNSW in 2010.

UMER AKRAM received the B.Sc. degree (Hons.) in electrical engineering from the COMSATS Institute of Information Technology, Abbottabad, Pakistan, in 2013, and the M.Sc. degree in electrical engineering from the King Fahd University of Petroleum and Minerals, Saudi Arabia, in 2018. He is currently pursuing the Ph.D. degree in electrical engineering from The University of Queensland, Australia. His current research interests include modern power system planning operation and design, optimization and control of distributed energy resources, demand side management, and energy storage systems.

SAIFULLAH SHAFIQ received the B.Sc. degree in electrical engineering from the University of Engineering and Technology, Lahore, Pakistan, in 2014, and the M.Sc. degree from the King Fahd University of Petroleum and Minerals, Dhahran, Saudi Arabia, in 2017. He is currently serving as a Lecturer with the Electrical Engineering Department, Prince Mohammad Bin Fahd University, Al-Khober, Saudi Arabia. His current research interests include power system planning, renewable energy resources, electric vehicles, power electronics, and demand side management.